SINGLET OXYGEN AND IODINE MONOFLUORIDE COLLISIONAL ENERGY TRANSFER MECHANISM

THESIS

Robert T. Mack
Captain, USAF

AFIT/GEP/ENP/89D-8

DEPARTMENT OF THE AIR FORCE
AIR UNIVERSITY
AIR FORCE INSTITUTE OF TECHNOLOGY

Wright-Patterson Air Force Base, Ohio

AFIT/GEP/ENP/89D-8

SINGLET OXYGEN AND IODINE MONOFLUORIDE COLLISIONAL ENERGY TRANSFER MECHANISM

THESIS

Robert T. Mack
Captain, USAF

AFIT/GEP/ENP/89D-8

Approved for public release; distribution unlimited

Preface

This research was part of an ongoing effort to characterize the energy transfer mechanisms between excited oxygen and interhalogen molecules. The specific goal of this work was to examine how $O_2(^1\Sigma)$ pumps vibrationally cold IF(X). Definition of the reaction and quantification of reaction rates will be critical to the development of high energy laser systems using these reactants.

I found the research rewarding in the knowledge and experience gained, and in working with the people who generously gave of their time. I would like to thank my advisor, Dr. Won B. Roh, for his encouragement and guidance and allowing me the opportunity to do this research. I would also thank my co-advisor, Capt Glen P. Perram for his direction and the many hours of drawing on his experience. I thank Dr. Ernest A. Dorko, WL/ARDJ, for sponsoring this thesis, and for his advice and encouragement on approaching problems. I am indebted to Mr. Greg Smith for his support with equipment, reactant gases, and the small problems that occurred daily. I thank Dr. Steven J. Davis for his conversation describing his experience with similar flowing apparatus. Finally, I thank God for the patience and perseverance of the last 18 months, and my wife, Kim, for her support and love through it all.

Robert T. Mack

Table of Contents

List of Figures

List of Tables

SINGLET OXYGEN AND IODINE MONOFLUORIDE COLLISIONAL ENERGY TRANSFER MECHANISM

I. Introduction

Background

The U.S. Air Force's interest in short wavelength chemical lasers has prompted interest in iodine monofluoride (IF) which emits in a region centered around 603 nm. One candidate pumping molecule for IF is singlet oxygen. While it has been experimentally demonstrated that singlet oxygen will pump IF (1-4), currently the pumping mechanism is not completely understood.

Electronic transitions in interhalogen molecules have long been identified. These systems hold potential for chemical lasers, providing that an efficient pumping scheme can be developed. The lifetime of IF(B) is long enough (approximately 7 μsec) to achieve large optical gain. Additionally, the Franck-Condon factors for IF(B$\rightarrow$X) are such that the transitions terminate on high v" levels, facilitating production of a population inversion between v'=0 and v"=4,5,6 (1:1). The first two electronically excited states of oxygen (O_2*) have been considered for pumping sources for lasers. The two states, $O_2(a^1\Delta_g)$ and $O_2(^1\Sigma_g^+)$ are metastable, the transition to the ground state is prohibited by the selection rules for optical dipole transitions (2:2). IF chemiluminescence due to O_2* pumping was

first observed in 1951 by Durie (2:3). Excited oxygen has been previously used to pump the atomic iodine laser system at AF Weapons Lab (Chemical Oxygen Iodine Laser). The combination of the two molecules, IF and O_2^* lends itself to being considered for a chemical laser system.

Problem Statement

The mechanism by which O_2^* pumps IF(X⟶B) has not been completely defined. To be pumped to the B-state, IF(X,v"=0 ⟶ B,v'=0) requires at least 18953 cm^{-1} of energy. The energy of the two O_2^* states are 7882 cm^{-1} for $O_2(^1\Delta)$, and 13121 cm^{-1} for $O_2(^1\Sigma)$. (v'=0 ⟶ v"=0) transitions. Clearly, a single O_2^* molecule doesn't have enough energy to pump IF(X) to the B state, and hence it is postulated that some multiple collision pumping scheme is involved. At least three $O_2(^1\Delta)$ molecules, or one $O_2(^1\Sigma)$ and one $O_2(^1\Delta)$ would be needed to pump IF(X⟶B) (1:6; 3:6797).

In addition to the pumping scheme, the lower level vibrational distribution of IF depends on the reactants used to produce IF. If CF_3I is used as an iodine source, the IF is produced essentially in a Boltzmann distribution where most of the molecules are in the lower v" levels. If I_2 is used, the distribution is bimodal, where a significant population is in the v"≥10. The two reactions are

$$CF_3I + F \longrightarrow IF(v"=0) \qquad (1)$$

$$I_2 + F \longrightarrow IF(v"\geq 10) \qquad (2)$$

and are labeled cold and hot reactions, respectively. IF produced

in the cold reaction requires more energy to reach the IF(B) state, needing to be pumped by an $O_2(^1\Sigma)$ and $O_2(^1\Delta)$ molecule, sequentially. The hot reaction gives enough vibrational energy to IF that it can be pumped to IF(B) by two $O_2(^1\Delta)$ molecules alone (2:6). The vibrational distribution for these two reactions are shown in Figures 1 and 2.

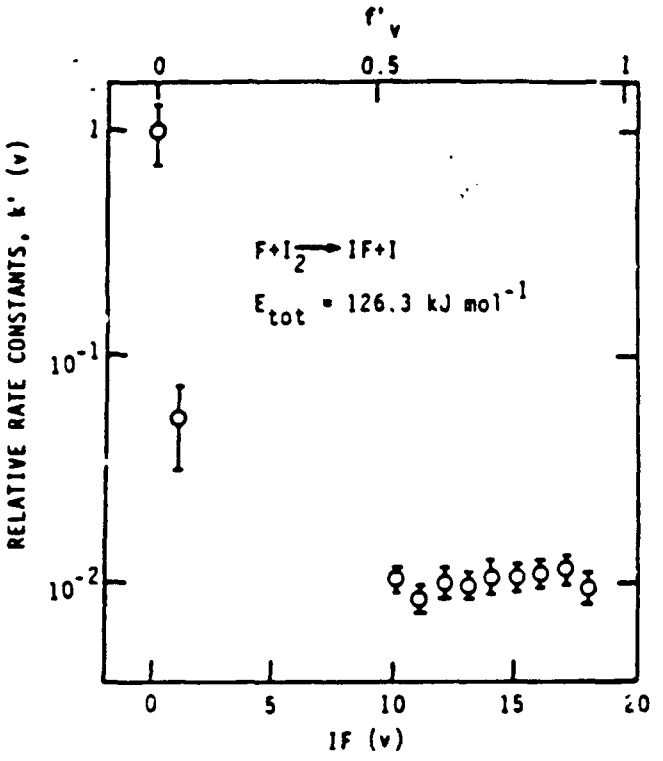

Figure 1. Detailed Rate Constants, k_v, for the Partitioning of Vibrational Energy in IF(X) Formed from F + I_2 (5:6508)

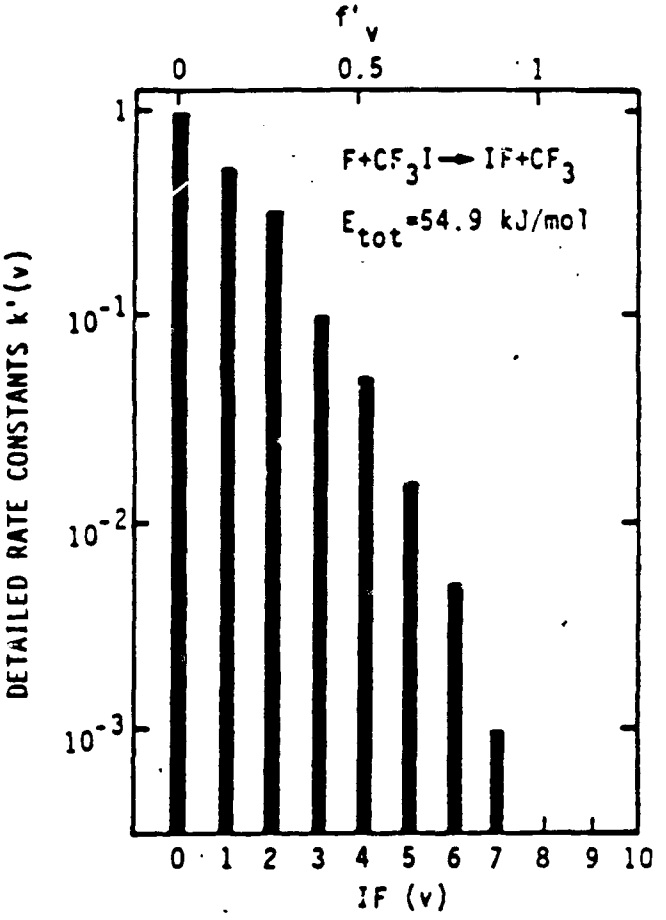

Figure 2. Detailed Rate Constants, k_v, for the Partitioning of Vibrational Energy in IF(X) Formed from F + CF_3I (6:1128)

Scope

This research will examine the effect of $O_2(^1\Delta)$ and $O_2(^1\Sigma)$ pumping vibrationally cold IF. This will entail several specific tasks:

- establish the presence of $O_2(^1\Sigma)$ in the reaction chamber
- measure the reduction in $O_2(^1\Sigma)$ emission as a function of reactant gas concentration
- from the reduction of $O_2(^1\Sigma)$ emission, determine the quenching coefficients of the reactant gases
- identify IF(B) production in the reaction chamber and examine the $O_2(^1\Sigma)$ pumping associated with it
- determine an upper bound on the rate constant of the $O_2(^1\Sigma)$ + IF(X) reaction.

Assumptions

The vibrational distribution of IF(X) produced in the cold reaction will be assumed to be comparable to the Boltzmann distribution determined by Stein and Wanner for the CF_3I + F reaction (6:1133). The O_2 and reactant gases used in the quenching experiments are assumed to be completely mixed and in steady state by the time they enter the reaction chamber.

Summary of current knowledge

Davis, et. al., showed that for vibrationally hot IF, the IF chemiluminescence intensity (and hence the IF(B) concentration, [IF(B)]) increased slightly as $[O_2(^1\Sigma)]$ was decreased. (The

square brackets [] denote concentration of the enclosed species). For vibrationally cold IF(X), the IF chemiluminescence intensity decreased as $[O_2(^1\Sigma)]$ decreased. This was suggestive that $O_2(^1\Sigma)$ is directly involved in pumping vibrationally cold IF, and that $O_2(^1\Delta)$ is the primary pumping molecule for vibrationally hot IF (1:15,23). In contrast to this, later work by Lee indicated contrary results; that for the cold reaction, [IF(B)] was not dependent on $[O_2(^1\Sigma)]$ (2:44-45). Both researchers did show that $O_2(^1\Delta)$ will pump vibrationally cold IF to the B state.

In either scheme, sequential pumping of IF by O_2^* requires pumping to some intermediate state. Davis, et.al. suggested $IF(A'\,^3\pi_2)$ (approximately 13,000 to 15,000 cm^{-1}) as the intermediate. $O_2(^1\Sigma)$ may pump IF(X,v=0) to IF(A'), or if IF(X,v"≥9) is present, then $O_2(^1\Delta)$ may have enough energy to pump it to IF(A') (1:6,3:6797).

The two reaction schemes are presented below:

For cold IF:

$$IF(X,v''=0) + O_2(^1\Sigma) \rightarrow IF(A') + O_2(^3\Sigma) \quad (3)$$

$$IF(A') + O_2(^1\Delta) \rightarrow IF(B) + O_2(^3\Sigma) \quad (4)$$

For hot IF:

$$IF(v''\geq 9) + O_2(^1\Delta) \rightarrow IF(A') + O_2(^3\Sigma) \quad (5)$$

$$IF(A') + O_2(^1\Delta) \rightarrow IF(B) + O_2(^3\Sigma) \quad (6)$$

Approach

Two experimental configurations were used for this research. The first series of experiments used a flow system similar to that

described by Lee (2:18). The reactants were mixed in a low pressure flowing reactor to form IF(B). The chemiluminescence was measured using a photomultiplier tube (PMT) and monochromator. The setup was modified to reduce the response time, minimize wall quenching in the O_2^* line, and to allow more precise control of the chamber pressure (7). Later experimental runs used a modified flow system where all the reactant gases could be injected into the O_2^* flow line. Mixing of the gases then occurred prior to entering in the reaction chamber. Similar to the work by Davis, et. al., the O_2^* flow was established first Reactant gases were then introduced in controlled quantities and the effect on $O_2(^1\Sigma)$ chemiluminescence intensity observed. From this data, the quenching rate coefficient could be determined.

II. Theory

Introduction

This chapter discusses the energy levels of iodine monofluoride and oxygen and their significance in assessing the excitation mechanisms. The energy transfer models of interest are described. Rate equations are derived and assessed under steady state conditions. A brief discussion on singlet oxygen and its quenchers is also included.

Iodine Monofluoride

The potential energy for the IF(X,v"=0 $\longrightarrow$ B,v'=0) transition is 18953 cm^{-1} (7:342). The Franck-Condon factors of the transition are such that a transition from a low lying v' level is more likely to terminate on a high lying v" level, leading to a natural population inversion. The potential energy curve for IF is shown in Figure 3. IF(X) produced by the reaction between CF_3I and F atoms has a vibrational distribution that is Boltzmann (5:1133). F atoms are produced by exposing CF_4 to a microwave discharge at 2450 MHz. Other research using similar conditions as will be used in this research determined that the exposed CF_4 flow contains undissociated CF_4, C_2F_6, atomic and molecular fluorine (the diagnostics were not sufficient to detect CF, CF_2 or CF_3). The ratio of [F] produced to the original [CF_4] was about 0.03. The ratio of [F_2] to [F] was about 0.1 to 0.3 (8:950).

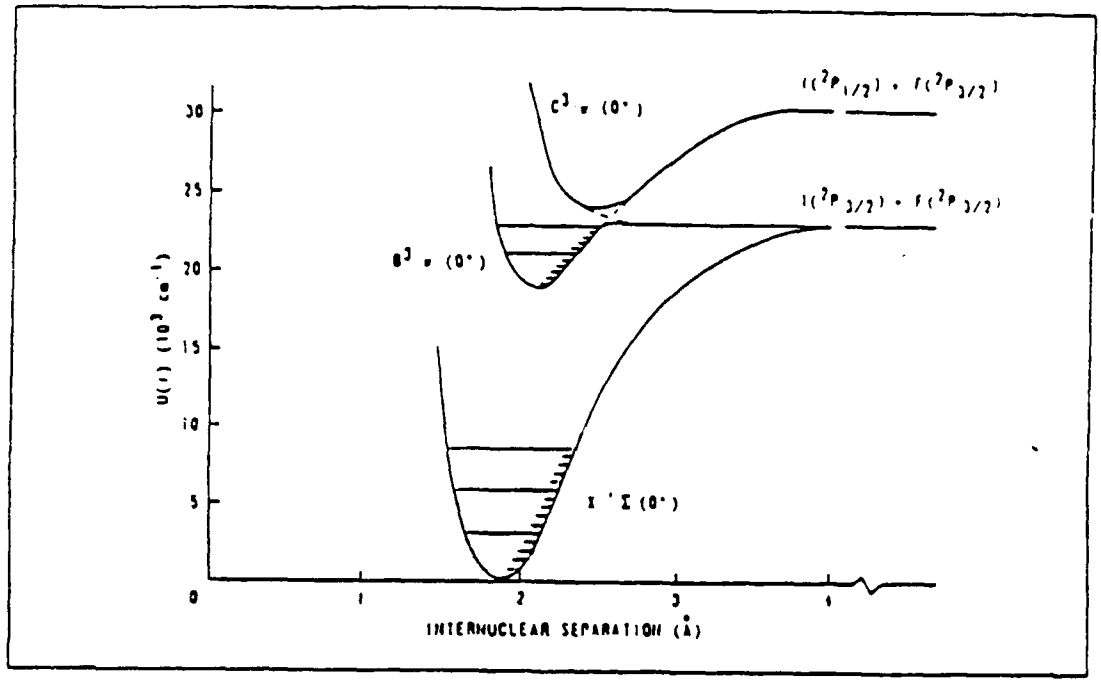

Figure 3. Potential Energy Diagram of IF (2:14)

Singlet Oxygen

Singlet oxygen refers to the first two electronic excited states of diatomic oxygen. The energy available from the $O_2(^1\Delta)$ and $O_2(^1\Sigma)$ molecules' v' = 0 to X, v'' = 0 transition is about 7882 cm^{-1} and 13121 cm^{-1}, respectively. The potential energy diagram of the levels are shown in Figure 4 (9:2).

It can be seen that one of either singlet oxygen molecules cannot provide enough energy to excite IF(X) to IF(B), but energy transfer from multiple singlet oxygen molecules could provide

sufficient energy. Depending on the initial vibrational IF(X,v") level, the intermediate IF state, and whether $O_2(^1\Delta)$ or $O_2(^1\Sigma)$ is involved in the energy transfer, electronic excitation may be achieved. A combined energy level diagram of IF and O_2 is shown in Figure 5 (1:6-7).

As much of this research dealt with singlet oxygen production and quenching, the following paragraphs discuss factors which determine the amount of $O_2(^1\Sigma)$ present during the reaction.

The first two excited states of singlet oxygen ($a^1\Delta_g$) and ($b^1\Sigma_g^+$) are both metastable, the transitions to the ground state ($X^3\Sigma_g^-$) being forbidden for electric dipole transitions. The transitions are nearly vertical, so transitions from low lying v' levels terminate on low lying v" levels. The two states have radiative lifetimes of approximately 45 minutes and 7 seconds, respectively, at zero pressure. At higher pressures, quenching due to collisions reduces the total (radiative + non-radiative) lifetimes (9:24).

Singlet oxygen can be produced by a number of means. Microwave discharge at 2450 MHz will produce approximately 5-15% $O_2(^1\Delta)$, and approximately 0.5-1.5% $O_2(^1\Sigma)$ (1:28). This initial $[O_2(^1\Sigma)]$ is quickly reduced by quenching, and at long times after the cavity, the $[O_2(^1\Sigma)]$ is determined by the pooling reaction of $O_2(^1\Delta)$. The steady state distribution is such that $[O_2(^1\Sigma)]/[O_2(^1\Delta)]$ is on the order if 10^{-3} (9:42). The quenching

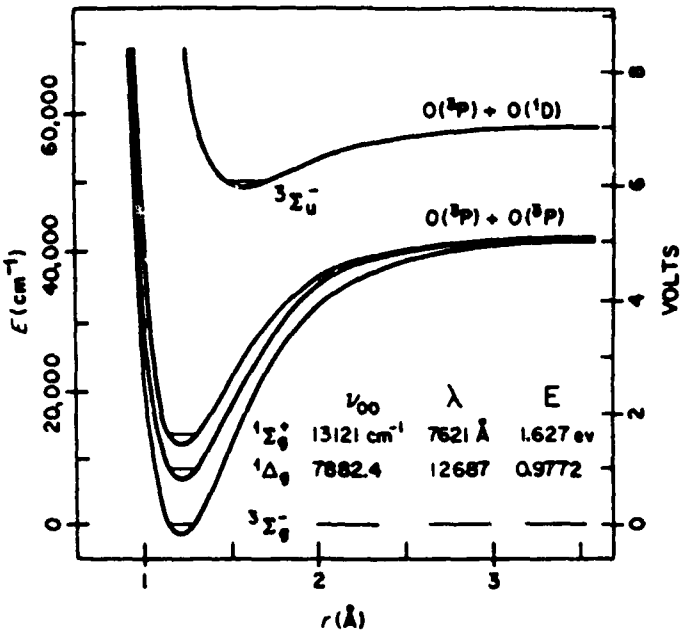

Figure 4. Potential Energy Diagram of O_2 (10:2)

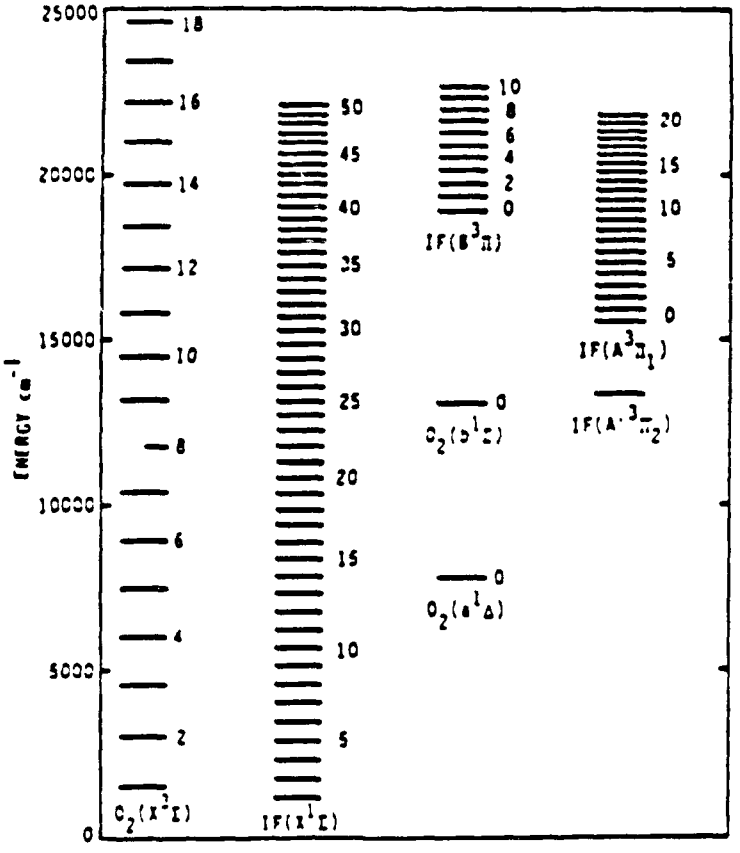

Figure 5. Energy Level Diagram of IF and O_2 (1:26)

and pooling reactions are described by the two equations:

$$O_2(^1\Sigma) + Q \rightarrow O_2(^1\Delta) + Q \quad (7)$$

$$O_2(^1\Delta) + O_2(^1\Delta) \rightarrow O_2(^1\Sigma) + O_2(X) \quad (8)$$

where the quencher here is $O_2(^3\Sigma)$.

The $O_2(^1\Delta)$ and $O_2(^1\Sigma)$ molecules differ markedly in the ease of deactivation. Removal of an $O_2(^1\Delta)$ by some quencher is a spin forbidden process, unless the quencher has multiplicity greater than 1 and can accommodate the 7882 cm^{-1} of energy liberated in the transition to $O_2(^3\Sigma)$. In contrast to this, quenching of $O_2(^1\Sigma)$ to $O_2(^1\Delta)$ is not a spin forbidden process, and liberates only 5239 cm^{-1} of electronic energy. These factors lead to most molecules quenching $O_2(^1\Sigma)$ about 10^5 as rapidly as $O_2(^1\Delta)$ (9:43).

Figures 6 and 7 give quenching coefficients for various molecules for $O_2(^1\Delta)$ and $O_2(^1\Sigma)$ (10:19,24). (To convert from $l/(mol\ sec)$ to $cm^3/(molecule\ sec)$ divide by 6.02×10^{20}).

Equations of Interest and Reaction Rates

A stated chemical reaction can be used to derive a rate expression for that chemical reaction. In general, a chemical reaction can be written as:

$$aA + bB \rightarrow gG + hH \quad (9)$$

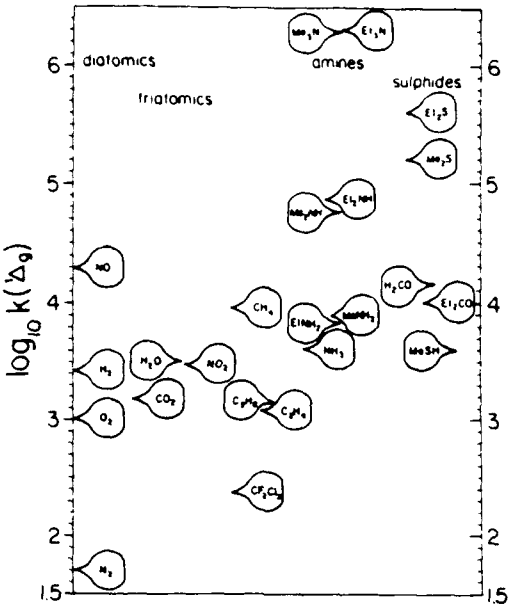

Figure 6. Logarithm of the Rate Constants for the Quenching of $O_2(^1\Delta_g)$ in units of 1 mol^{-1} s^{-1} (11:19)

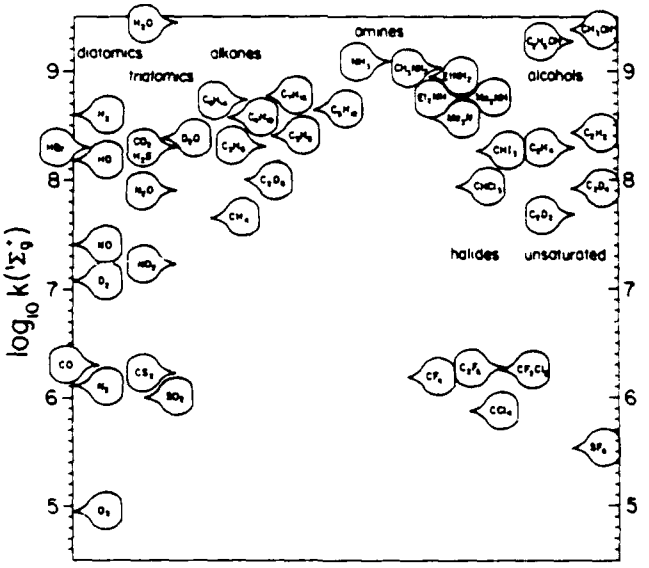

Figure 7. Logarithm of the Rate Constants for the Quenching of $O_2(^1\Sigma_g^+)$ in units of 1 $mol^{-1}s^{-1}$ (11:24)

The rate of the reaction may be expressed in terms of the rate of disappearance of reactants or rate of appearance of products:

$$-\frac{d[A]}{dt}, -\frac{d[B]}{dt}, \frac{d[C]}{dt}, \frac{d[D]}{dt} \qquad (10)$$

The signs are chosen such that the rates are positive.

As the reaction may use or produce different concentrations of reactants or products, the rate of change of the concentrations for the above reaction is:

$$-\frac{1}{a}\left[\frac{d[A]}{dt}\right] = -\frac{1}{b}\left[\frac{d[B]}{dt}\right] = \frac{1}{c}\left[\frac{d[C]}{dt}\right] = \frac{1}{d}\left[\frac{d[D]}{dt}\right] \qquad (11)$$

(12:9).

The rate for the reaction then is defined as

$$\text{rate} = k\,[A]^{n_1}\,[B]^{n_2}\ldots \qquad (12)$$

where k is the rate constant, with the units of $[\text{conc.}]^{1-n}$ $[\text{time}]^{-1}$. The order of the reaction is "n", where $n = n_1 + n_2 + \ldots$, simply the sum of the exponents. Each exponent is the order with respect to that component (12:10,11).

Rate constants are determined experimentally. By plotting the change in concentration of a species verses time elapsed since the start of the reaction, the time rate of change of the concentration can be found. The rate is simply the negative of the slope of the curve at a particular point. The rate constant k can then be found from the rate equation (12) (13:379-380).

There are many reactions occurring which determine $[O_2(^1\Sigma)]$, which in turn can then pump vibrationally cold IF(X). The

reactions of interest, and assumed to be the predominant reactions are listed below.

$$O_2(^1\Delta) + O_2(^1\Delta) \xrightarrow{k_p} O_2(^1\Sigma) + O_2(^3\Sigma) \quad (13)$$

where $k_p = 2 \times 10^{-18}$ cm^3 molecule^{-1} s^{-1} (10:41).

$$O_2(^1\Sigma) \xrightarrow{1/\tau} O_2(^3\Sigma) + h\nu \qquad \lambda = 762 \text{ nm} \quad (14)$$

τ = 7 seconds (radiative lifetime).

$$O_2(^1\Sigma) + O_2(^3\Sigma) \xrightarrow{k_{3_\Sigma}} O_2(^1\Delta) + O_2(^3\Sigma) \quad (15)$$

$k_{3_\Sigma} = 3.9 \times 10^{-17}$ cm^3 molecule^{-1} s^{-1} (15:18).

$$O_2(^1\Sigma) + M \xrightarrow{k_M} O_2(^1\Delta) + M \quad (16)$$

where M = CF_4, F, CF_3, IF, etc, and $k_{CF_4} = 2.6 \times 10^{-15}$ cm^3 molecule^{-1} s^{-1} (11:24).

$$O_2(^1\Sigma) + \text{wall} \xrightarrow{k_w} O_2(^1\Delta) \quad (17)$$

$$O_2(^1\Sigma) + Q \xrightarrow{k_Q} O_2(^1\Delta) + Q \quad (18)$$

Q is a contaminant present in the O_2 or quencher gas, and [Q] is proportional to [O_2] or [M]. P is the partial pressure of the gas.

The $O_2(^1\Sigma)$ in the reaction chamber is produced by the pooling reaction of $O_2(^1\Delta)$, equation (13). This reaction is fairly slow, and the $O_2(^1\Delta)$ concentration is assumed to be large relative to the $O_2(^1\Sigma)$ concentration. Competing with this reaction are the

reactions that reduce the $O_2(^1\Sigma)$ concentration. The $O_2(^1\Sigma)$ will spontaneously emit at 762 nm, equation (14). Non-radiative processes also occur, some of which have been characterized by previous research. Quenching by ground state oxygen occurs, equation (15). Quenching also occurs by molecular collisions with other gases such as IF or its precursors, CF_4 and CF_3I, equation (16). Collisions with the tubing walls will also quenching the $O_2(^1\Sigma)$ molecules. If the concentrations of the reacting species are known, then the concentration of $O_2(^1\Sigma)$ can be found (14, 15).

At long times, $O_2(^1\Sigma)$ is produced by the pooling reaction of $O_2(^1\Delta)$. Assuming a fixed efficiency for production of $O_2(^1\Delta)$, the $O_2(^1\Sigma)$, $O_2(^1\Delta)$ and $O_2(^3\Sigma)$ concentrations can be related to the total O_2 concentration by

$$[O_2(^3\Sigma)] = f_1[O_2] \qquad f_1 \cong 0.9 \qquad (17)$$

$$[O_2(^1\Delta)] = f_2[O_2] \qquad f_2 \cong 0.1 \qquad (18)$$

$$[O_2(^1\Sigma)] = f_3[O_2] \qquad f_3 \cong 10^{-4} \qquad (19)$$

If the gases contain impurities, then the effects of these must be taken into account in the quenching rate. If the O_2 contains a finite amount of contaminant, this will then affect the ground state oxygen quenching rate. What will be measured is a rate that is a sum of the oxygen quenching rate and the contaminant quenching rate. The effect of the contamination can be expressed in an effective quenching rate in terms of the O_2 concentration. The contaminant concentration can be expressed as

$$[Q] = a[O_2] = (a/f_1)[O_2(^3\Sigma)] \tag{20}$$

then

$$k_{3_\Sigma}[O_2(^3\Sigma)] + k_Q[Q] = \left[k_{3_\Sigma} + \frac{a\,k_Q}{f_1}\right][O_2(^3\Sigma)] \equiv k'_{3_\Sigma}[O_2(^3\Sigma)] \tag{21}$$

In similar fashion for a contamination present in the quencher gas

$$[Q] = b[M] \tag{22}$$

$$k_M[M] + k_Q[Q] = (k_M + b\,k_Q)[M] \equiv k'_M[M] \tag{23}$$

Steady State Analysis of $O_2(^1\Sigma)$ Quenching

The rate of change in concentration of a reactant or product is related to the concentration of those species which determine its production or removal as:

$$\frac{d[\text{species}]}{dt} = +\sum k_{prod}[\text{react}]^{coeff} - \sum k_{remove}[\text{react}]^{coeff} \tag{24}$$

For the above reactions which involve $O_2(^1\Sigma)$ (equations (13), (15), (16) and (17)), this gives

$$\frac{d[O_2(^1\Sigma)]}{dt} = k_p[O_2(^1\Delta)]^2 - (k'_M[M] + k'_{3_\Sigma}[O_2(^3\Sigma)] + k_w)[O_2(^1\Sigma)] \tag{25}$$

At long times, this process comes to a steady state, so d[ ]/dt = 0, and the equation becomes

$$[O_2(^1\Sigma)]_{ss} = \frac{k_p\,[O_2(^1\Delta)]^2}{k'_{3_\Sigma}[O_2(^3\Sigma)] + k'_M[M] + k_w} \tag{26}$$

Making the substitutions from equations (17) and (18) into (26), this can be rewritten

$$[O_2(^1\Sigma)]_{ss} = \frac{k_p f_2^2 [O_2]^2}{k'_{3_\Sigma} f_1 [O_2] + k'_M [M] + k_w} \quad (27)$$

From this equation, it is seen that for a given concentration of $O_2(^1\Delta)$, addition of M will reduce $O_2(^1\Sigma)$. If the concentrations of $O_2(^1\Delta)$, $O_2(^3\Sigma)$, $O_2(^1\Sigma)$ and quencher M are known, then k_M can be determined.

If the concentration of $O_2(^1\Sigma)$ cannot be measured or determined from the $O_2(^1\Sigma)$ emission, then the data can be normalized relative to the $O_2(^1\Sigma)$ emission when no quenching gas is present

$$[O_2(^1\Sigma)]^* = \frac{k_p f_2^2 [O_2]^2}{k'_{3_\Sigma} f_1 [O_2] + k_w} \quad (28)$$

The ratio of the two emission intensities is

$$\frac{[O_2(^1\Sigma)]^*}{[O_2(^1\Sigma)]_{ss}} = \frac{k'_{3_\Sigma} f_1 [O_2] + k_w + k'_M [M]}{k'_{3_\Sigma} f_1 [O_2] + k_w} \quad (29)$$

$$= 1 + \frac{k'_M [M]}{k'_{3_\Sigma} f_1 [O_2] + k_w} \quad (30)$$

For convenience, the following quantities are defined:

$$\beta = \frac{k'_M}{k'_{3_\Sigma} f_1} \tag{31}$$

$$\gamma' = \frac{k_w/[O_2]}{k'_{3_\Sigma} f_1} \tag{32}$$

$$\frac{[O_2(^1\Sigma)]^*}{[O_2(^1\Sigma)]} = \frac{I_{M=0}}{I_M} \equiv S \tag{33}$$

$$\frac{[M]}{[O_2]} = \frac{P(M)}{P(O_2)} \tag{34}$$

where I is the emission intensity. The final rate equation is then

$$S = 1 + \frac{\beta\,([M]/[O_2])}{1 + \gamma'} = 1 + \frac{\beta}{1 + \gamma'} \times \frac{P(M)}{P(O_2)} \tag{35}$$

which is a linear equation. A plot of S verses the ratio of the partial pressures of the gases will ideally produce a straight line with a slope of $\beta/(1 + \gamma')$ and intercept of 1 (14). The gas quenching information is contained in β. Contaminants with a $k_Q > k_M$ present in M will increase the value of β (increase the line slope). In similar manner, contaminants in the O_2 with $k_Q > k_{3_\Sigma}$ will decrease β (decrease the slope) and reduce the apparent value of k'_M. A large wall rate γ' will decrease the overall slope term, and if not accounted for will reduce the apparent value of k'_{3_Σ} (14).

The wall quenching is defined as

$$k_w = \gamma \frac{A_s}{V} \frac{\bar{c}}{4} \tag{36}$$

where γ is the quenching efficiency (not to be confused with γ', the normalized wall quenching term), A_s is the surface area, V is the volume, and $\bar{c}$ is the mean thermal velocity. Mean thermal velocity is defined as

$$\bar{c} = \left(\frac{8\ k\ T}{\pi\ M}\right)^{1/2} \tag{37}$$

where k is Boltzmann's constant, T is temperature, and M is the mass of the gas (in this case, O_2) (14).

In this development, several assumptions were made. These are listed below.

- The O_2 pressure is held constant during the quenching experiments. It is assumed that the $O_2(^1\Delta)$ concentration is constant during the quenching experiments. Most gases' quenching coefficients for $O_2(^1\Sigma)$ are about 10^5 faster than those for $O_2(^1\Delta)$ (10:19,24,34). In view of this fact, this assumption appears reasonable.

- The $O_2(^1\Sigma)$ concentration in the viewing region is assumed to be determined by the $O_2(^1\Delta)$ pooling reaction. The initial $O_2(^1\Sigma)$ concentration produced by the microwave discharge is assumed to have been quenched out prior to the viewing region. The extent to which this is true will be determined by the gas flow speed (residence time in the tubing prior to the viewing region), the wall quenching, and the concentration of quenching gas in the system.

- The $O_2(^1\Sigma)$ is assumed to be quenched to $O_2(^1\Delta)$, rather than

to $O_2(^3\Sigma)$. This assumption is typical in $O_2(^1\Sigma)$ rate coefficient research (14, 16:453). Additionally, there was no rate available for the deactivation of $O_2(^1\Sigma)$ to $O_2(^3\Sigma)$.

- All of the reacting species are assumed to be in steady state by the time the gases enter the viewing region.

III. Experimental Apparatus

Introduction

This section describes the experimental apparatus used in this research. The major components of the system are the flowing reactor used to contain the $O_2(^1\Sigma)$ + IF(X) and the collection/recording system used to record and measure the emission of the spectrum.

Flowing Reactor System

The flow system consists of the following components:

Six-way Cross (reaction chamber)

Flowmeters

Plumbing and reactants

Vacuum System.

Six-way Cross. The reaction chamber was a six-way cross which contained the O_2^* + IF or O_2^* + quencher reaction. In the initial runs, the cross had two plexiglass ports which allowed viewing of the flame and illumination of the monochromator slit. The four remaining ports were covered with stainless steel plates with 1/2 inch Cajon feed-through connectors welded in place. The vacuum system, Baratron pressure manometer, oxygen inlet tube, and IF inlet tube were installed through the Cajon connectors. The initial flowing reactor system is shown schematically in Figure 8. The vacuum system was connected to the top of the chamber by 1/2 inch outer diameter (OD) copper pipe. The Baratron pressure gauge was a capacitance manometer type, 200 series, with a pressure

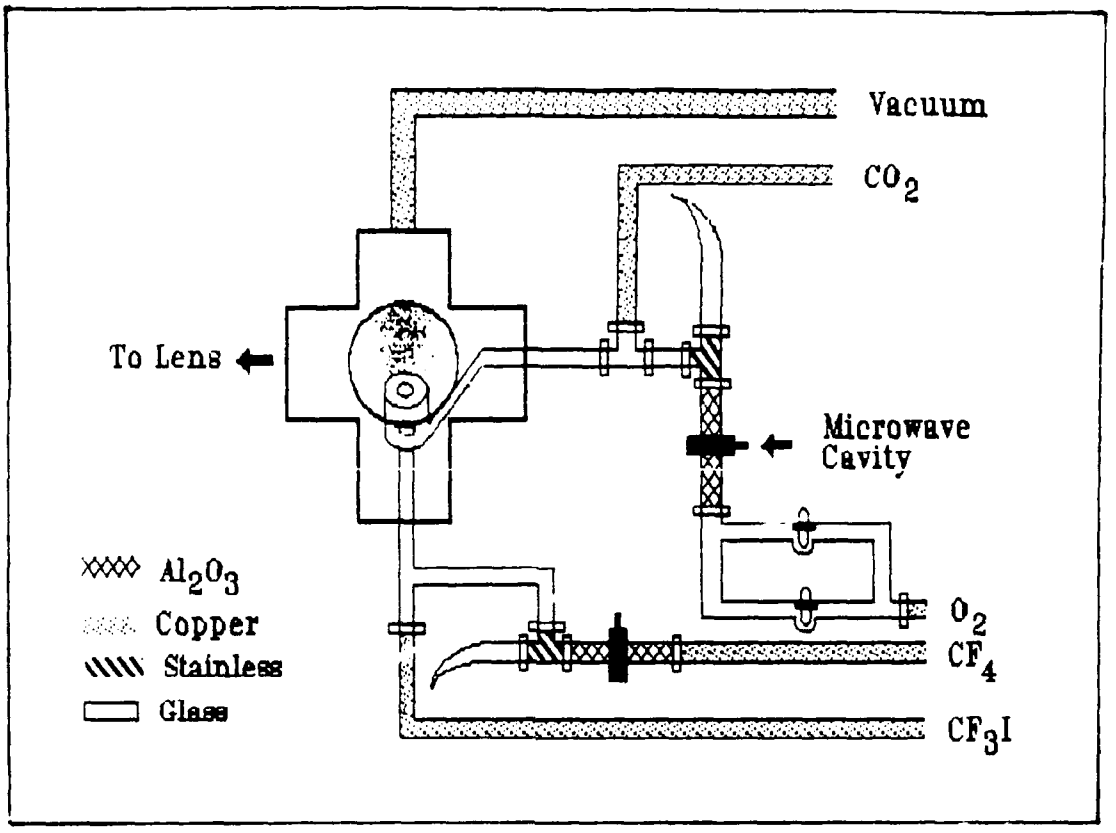

Figure 8. Schematic Diagram of Initial Flowing Reactor System

range of approximately 0.01 torr to 100 torr. A digital voltmeter was connected to the analog gauge to facilitate reading the total pressure. For the IF(B) emission, the oxygen inlet entered the chamber through one side port, with the IF inlet tube being brought in through the bottom port. For $O_2(^1\Sigma)$ quenching runs, the system was reconfigured to bring the IF inlet tube directly into the O_2 line. The bottom steel plate/Cajon feed through connector was then replaced by a solid steel plate.

Flowmeters. The reactant and quenching gases were controlled with one of two different Airco flowmeters (type SS754 and SS756) depending on the required flow rate of the gases. Each flowmeter contained both a glass and stainless steel metering ball (float) to allow metering over a large dynamic range. The SS754 tubes will meter flows from 20-760 standard cubic centimeters per minute (sccm). The SS756 tube will meter flows of 100-4800 sccm (2:18-19). The SS754 tubes were used for CF_3I, CF_4, CO_2 and N_2, and the SS756 tubes used to control the O_2 and He gases. The flowmeters provide an indication of the relative proportions of the gases, and with calibration curves, are used to calculate the flow velocity (14, 17).

Plumbing and Reactants. The high pressure gas supply cylinders were connected to the flowmeters by 1/4 inch OD copper tubing. The cylinder regulators were set to supply 5 to 8 psig. The flowmeters were then connected to the other system components using 1/4 inch OD copper tubing. Swaglock connectors are used for metal-to-metal connections, Cajon connectors are used for connections to glass or ceramic pieces. Each of the gas line components will be discussed below.

The main oxygen flow is connected to a dual valve system prior to entering the microwave cavity. One branch of the system contains a mercury reservoir. The reservoir is opened prior to a run, which allows mercury vapor to flow through the microwave cavity. This creates a ring of mercuric oxide (HgO) which coats the inside of the oxygen inlet tube. The HgO ring removes atomic

oxygen (created in the microwave discharge region) which could otherwise affect the IF(B) chemistry. The mercury reservoir is closed during actual experiments to prevent mercury from entering the oxygen inlet bowl. During the $O_2(^1\Sigma)$ quenching experiments, the system was no longer coated with HgO. This practice had no apparent effect on the $O_2(^1\Sigma)$ concentration. The oxygen then travels to a 1/2 inch OD aluminum oxide tube where it is exposed to the 2450 MHz, 120 watt microwave cavity. The cavity was typically run at 60 watts forward power. The microwave cavities used in this case are Evenson type cavities. Operating microwave cavities will heat up with time and become unstable. The cavities were cooled using compressed air blown through 1/4 inch plastic tubing and circulated via the cavity cooling port. Additionally, a small fan blew air past the cavities which aided in the cooling. The air flow was enough to keep the cavities warm to the touch, which also kept the cavities stable with respect to the reverse power over several hours. (While the cavity tuning remained constant, the power output of one power supply initially used for O_2 did appear to vary cyclically over a minute. The supply was switched with the other (CF_4) cavity power supply, as the $[O_2(^1\Delta)]$ stability was more critical).

Additionally, the cavity discharge region produced visible light, so a light trap ("Wood's Horn") was installed in the O_2 line prior to its entering into the reaction chamber. To further reduce stray light, an opaque barrier was installed around the chamber, between the cavities and the optical system.

Finally, the oxygen was injected into the cavity through a mixing bowl which consisted of a hollow cylindrical structure with holes drilled into the inside wall. The oxygen traveled into the hollow section and was injected into the chamber via the holes.

IF(X) is produced from fluorine atoms (F) and iodotrifluoromethane (CF_3I). Fluorine atoms are produced by passing tetrafluoromethane (CF_4 or Freon 14) through a microwave discharge cavity and light trap assembly similar to the O_2 line. This technique produces fluorine atoms and various other carbon-fluorine radicals. These gases are then mixed with CF_3I gas in a glass tee immediately below the reaction chamber. The fluorine atoms react with the CF_3I to produce IF(X) and CF_3 (6:1128). The glass tee is coated with halocarbon wax to prevent IF(X) from forming IF_3 and IF_5 via wall collisions (4:37). The IF(X) travels up the glass tee to the base of the oxygen inlet bowl where it reacts with the singlet oxygen to produce IF(B).

For the $O_2(^1\Sigma)$ quenching experiments, the system was reconfigured to introduce all the gases into the O_2 line prior to entering the reaction chamber. This provided similar mixing conditions for all of the quenching gases. The IF tee was removed from the bottom of the chamber and joined to the O_2 line prior to its entering the chamber, allowing introduction of CF_3I or microwave CF_4 into the O_2 line. This occurred approximately 25 cm prior to injection into the cavity. Helium gas and CO_2 were introduced into the O_2 flow through a side arm upstream of the IF tee. The modified flow system is shown schematically in Figure 9.

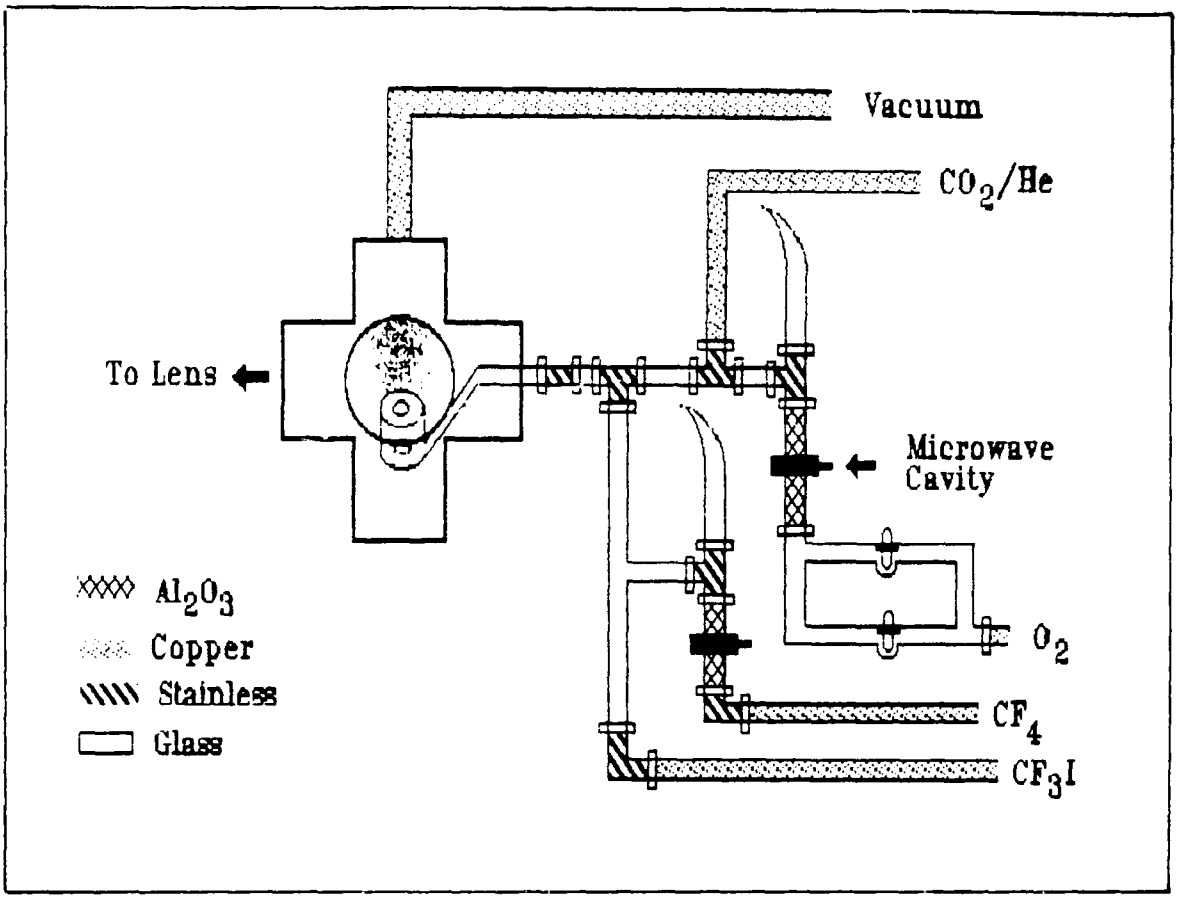

Figure 9. Schematic Diagram of Modified Flowing Reactor System

The gases used in this work were of varying degrees of purity. The O_2 used was ultra high purity, 99.98% minimum (18:54). The CF_4 used was 99.7% purity (18:33). CF_3I obtained from PCR Corporation was 99% purity. Other researchers using CF_3I from PCR indicated that the major contaminants in the gas were I_2 (19:10), N_2 and O_2 (20). The CF_3I was used without purification. The helium gas was labeled as "high purity, oil free", but on inquiry it was found that the gas cylinder was filled from a railroad tank car which was also used to transport nitrogen gas

(21). The helium was assumed to be contaminated, and quenching data associated with it was taken to be suspect. The CO_2 purity was not identified, but as the CO_2 quenching rate was so large, contaminants were assumed to have minimum noticeable effect on the CO_2 quenching data. N_2 gas used was ultra high purity, grade 5 (99.999% pure).

Vacuum. The vacuum system consists of a Sargeant-Welch, model 1375 vacuum pump with a free-air displacement capacity of 1000 liters per minute. A large ball valve at the pump intake is used to isolate the pump from the system. The ball valve is left fully open during runs. The reaction chamber is connected to the vacuum pump by 1/2 inch OD copper tubing, connected to a 1/2 inch butterfly valve which allows fine control of the flow from the chamber to the pump. One inch OD stainless steel tubing connects the butterfly valve to the ball valve.

Optical analysis and Recording System

The optical collection and recording system is shown schematically in Figure 10. The IF(B) chemiluminescence flame/$O_2(^1\Sigma)$ emission is imaged onto the monochromator slit by two 15 cm focal length lenses, one with the emission at its focal length and the other with the entrance slit at its focal length. The monochromator is a 0.3 meter McPhearson scanning monochromator with a 1200 lines-per-mm grating. Located at the monochromator exit slit is an RCA C310134-02 photomultiplier tube (PMT) inside a thermoelectrically refrigerated housing at -20°C. The PMT has a

gallium arsenide photocathode with a spectral response from 250 to 850 nm (7, 22).

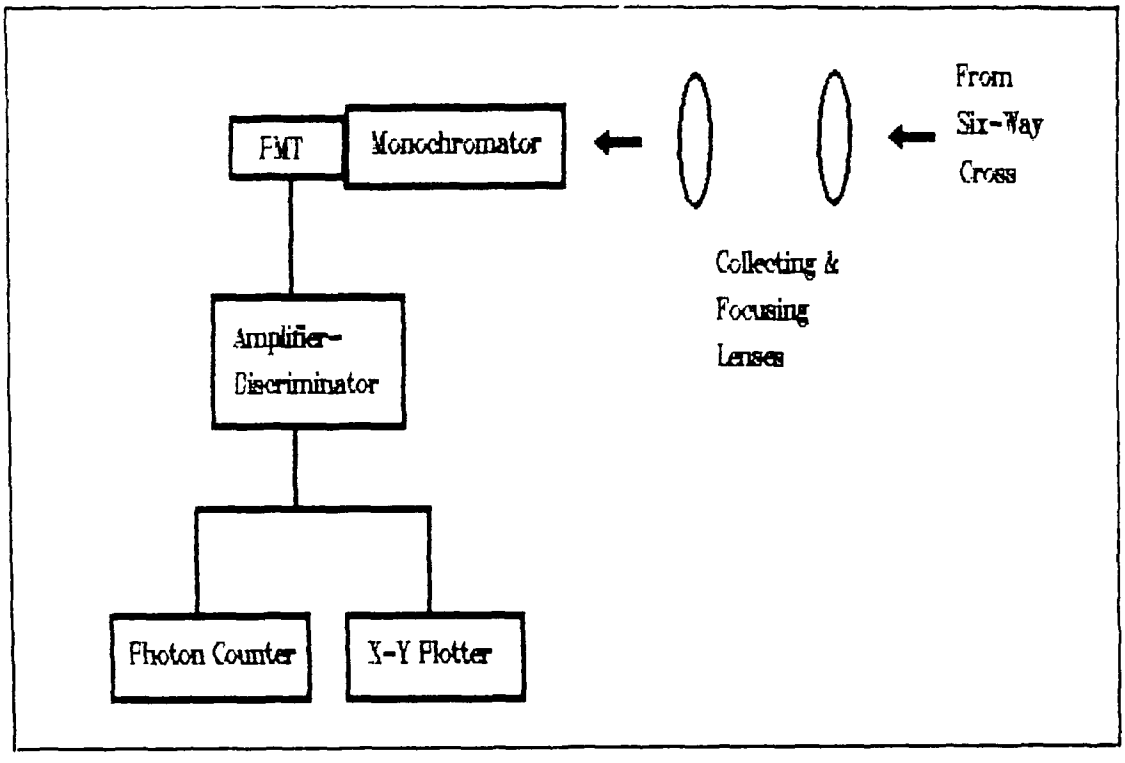

Figure 10. Schematic Diagram of Optical Analysis and Recording System

The PMT output is connected to an amplifier-discriminator and photon counter system. An EG&G Princeton Applied Research model 1121A Amplifier Discriminator supplies the bias voltage to the PMT and controls the signal threshold level used to obtain the best signal to noise ratio. The Discriminator Control Unit module of the Amplifier Discriminator contains a digital and positive analog voltage output. The digital output is connected to an EG&G Model

1112 Photon Counter/Processor, which displays the photon count per second at the spectral location selected by the monochromator. The analog output is connected to a Soltec strip chart recorder. The positive analog output voltage varies linearly with the count rate, so the chart recorder records the relative intensity of the IF(B) emission as the monochromator scans the spectrum. A 50 microfarad capacitor is installed between the positive and negative signal inputs of the recorder to help reduce the noise (7). The strip recorder was used in the early stages of the research to identify IF(B) emission. During $O_2(^1\Sigma)$ quenching runs, the monitoring relied mainly on only the photon counter as the recording diagnostic, however, the strip recorder was used during some of the quenching runs to record the time evolution of the $O_2(^1\Sigma)$ emission as a function of the quencher pressure. This was useful in identifying how and when the system came to equilibrium.

IV. Experimental Procedures.

Introduction

This section describes the procedures used for the two experimental objectives: 1) to produce IF(B) emission and collect emission spectra, and 2) produce and quench $O_2(^1\Sigma)$ emission and record the changes in emission intensity. The general procedures are discussed first, then aspects unique to each experiment will be discussed.

Routine Start Up

Prior to a run, the system is pumped down to the limits of the pump, usually 0.01 torr. Higher pressures indicate a leak, dirty pump oil, or degassing within the system. Both the ball valve and butterfly valve are opened completely. Once the desired pressure is achieved, the butterfly valve is closed, and the pressure observed to check for signs of a leak. (A tolerable leak would increase the pressure on the order of 0.5 torr/hour). The butterfly valve is then fully opened to again evacuate the system. The ball valve is left fully opened, and is closed only to isolate the pump from the system when the pump is shut off. The butterfly valve was open to 3/4 of a turn. This allowed a flow velocity of approximately 0.7 m/sec, measured in the gas tubing prior to entering the reaction chamber.

IF Emission

The CF_4 flowmeter is opened until the chamber pressure reads

0.8 torr on the digital voltmeter. The compressed air cooling the cavities is turned on, the cavity is lit, and CF_4 allowed to flow for a few minutes prior to flowing O_2. The O_2 flowmeter is then adjusted until the pressure reads 1.6 torr. Lighting the cavities is occasionally difficult. The power is initially turned to zero, and while "tickling" the cavity with the Tesla coil, the power is slowly increased until the cavity lights or the forward power reaches 60 watts. If the cavity does not light, it may be necessary to rotate the tuning screw and slide/rotate the tuning rod a bit, or reducing the gas pressure to around 0.5 torr. Once a cavity is lit, it is tuned with the tuning screw and tuning rod until the reverse power is between 0 and 3 watts. The compressed air flow is adjusted to cool the cavities such that they are warm to the touch. The aluminum oxide tube will become hot, but the cooled cavities will generally remain stable with respect to the forward and reverse power. The reverse power will change with the gas flow through the tube and the chamber pressure.

Occasionally, the microwave cavity will arc instead of lighting. If this occurs, the power is reduced to zero (to stop the arcing and not arc through the tube), and the cavity is relit. Arcing may be due to the connection between the cavity and power cable not being tight or the connections inside the connector not being in contact.

Initially, the oxygen aluminum oxide tube was coated with HgO prior to a day's operation. The HgO ring appeared as a dark brownish ring inside the aluminum oxide tube approximately 2 cm

downstream of the cavity. As described in the background section, this was expected to have the effect of reducing the atomic oxygen. However, the atomic oxygen peak at 777.1 nm did remain fairly strong (the intensity was on the same order as that of the $O_2(^1\Sigma)$ emission at 762 nm). The atomic oxygen didn't appear in any significant concentrations that adversely affected the IF(B) or $O_2(^1\Sigma)$ emission, and this practice was discontinued (14, 23).

A small amount of CF_3I was then introduced into the flow. The partial pressure was on the order of 0.01 to 0.03 torr. The gas flows were adjusted to maximize the emission at 762 nm. The IF(B) emission spectrum was obtained at the following partial pressures: $P(CF_4)$ = 2.41 torr, $P(O_2)$ = 0.54 torr, and $P(CF_3I)$ = 0.01 torr.

Special Considerations

If the system was opened to ambient air, the system needed to be pumped down for a period ranging from 1/2 hour to a few days. During the first half hour, the pressure would quickly fall to 0.4 torr, then drop more slowly to 0.01 torr. Over the longer period, outgassing would occur, the degree of which had a substantial effect on $O_2(^1\Sigma)$ emission. The biggest factor affecting $[O_2(^1\Sigma)]$ was system cleanliness. This was achieved simply by constantly keeping the system under vacuum for extended periods of time. For experiments involving microwave CF_4, the system would need to be passivated by running CF_4 through the discharge for an hour prior to actual experiments (23).

IF(B) Chemiluminescence Spectral Analysis

The monochromator was initially set to 603 nm (B, v'=0 $\rightarrow$ X, v''=4 transition) with 2 mm slits. This provided the maximum signal to noise ratio and was used to adjust the gas mixtures to optimize the flame.

Dark counts were obtained by closing the shutter, and were typically about 10/sec. Background counts were taken with the shutter open, prior to adding the CF_3I to the flow.

The strip recorder was typically set to 2 or 4 cm/min. The recorder was started with the mode selected to record the zero position. The monochromator was set to begin scanning at the shorter wavelength at a scan rate of 20 nm/min, the plotter's mode is switched from "zero" to "on" while noting the wavelength reading of the monochromator. At the end of the spectrum recording, the recorder is switched from "on" to "zero" at the desired wavelength reading of the monochromator. In switching from "zero" to "on", a vertical displacement is produced on the paper.

For precise wavelength identification, emission from Oriel pen lamps were recorded using the monochromator and the difference between true and measured wavelength determined. Calibration corrections varied from 0.4 to 0.6 nm depending on the monochromator spectral location and slit width.

Quenching Experiments

The system was modified for $O_2(^1\Sigma)$ quenching as described earlier. This had the advantage of creating roughly the same

mixing conditions for each quencher gas. Unfortunately, this arrangement precluded any possibility of varying the reaction time or mixing time, but it was more conducive to having the flow reach steady state by the time it reached the reaction chamber. As there were not enough SS754 flowmeters for each gas, there was a need to disconnect an existing gas line to connect a new line. Prior to a run, (particularly if the system had been opened or if a supply gas line to a flowmeter was changed) the system was pumped down for several minutes. If no gas lines were changed, the reaction chamber was simply evacuated. If gas lines were changed, the regulators were closed, the flowmeters opened, and the lines evacuated to remove contaminants. The butterfly valve was left 1/4 turn open for most of the runs, however a few runs were done for which the valve was set at 1/8 turn open. The O_2 pressure was increased to one torr and the O_2 microwave cavity lit. It was found that the $O_2(^1\Sigma)$ emission (photon count) took a few minutes to stabilize. Once this occurred, the O_2 pressure was increased to 2.5 or 4 torr, depending on the run. With the valve 1/4 turn open and 4 torr total pressure in the reaction chamber, the gas velocity was on the order of 0.3 m/sec.

A quenching experiment then consisted of slowly increasing the quencher pressure in small increments (usually 0.005 torr or less) and recording the $O_2(^1\Sigma)$ photon count. Quencher pressure was increased to a maximum of 0.5 torr. This was low enough to allowed the O_2 flow to remain essentially the same (to within three percent of its initial pressure). Counts were taken by

sampling over a 10 second interval with the photon counter/processor, then dividing the count by ten. Additionally, ample time was allowed for the count to stabilize.

Later runs were done by increasing the quencher pressure in interrupted increments, that was to increase the pressure, reduce it to zero, increase the pressure to a higher value, reduce it to zero. This provided a photon count due to the quencher contaminated walls and gave a measure of the change in the wall quenching effect.

Some measure of the reaction between the tubing wall and the quencher gas was attempted by comparing the system before and after exposure to the quenching gases. The system was evacuated, the valves closed and the pressure rise due to system leaks monitored. The system was then filled with gas to a few tenths of a torr, closed off, and the pressure again monitored. The system was then evacuated, closed off, and the pressure monitored.

The Baratron was found to be in need of calibration. Absolute pressure readings were inaccurate (negative pressure readings were displayed while gas flow was evident), but pressure differences were assumed to be accurate. This problem most affected the O_2 flow, as that was usually the first (and largest) flow to be established. A second problem was that the smaller flowmeter (SS754) took longer to stabilize than the larger flowmeter. If sufficient time was not allowed for the meter reading to stabilize, the flowmeter tended to drift slowly shut. It did appear that the meter reading reproduced approximately the

same pressure whether a pressure was established manually or by the drift. An estimate of the error introduced by both of these problems was used to calculate error bounds for the experimental quenching rate coefficients.

V. Results and Discussion

Introduction

The following section presents results of the work and compares them with previous work or literature data. Where possible, explanations are given for discrepancies, and suggestions are made for improvement.

IF(B) Emission

The IF(B) emission spectrum is shown in Figure 11. Transitions have been assigned. The most intense peaks are those due to the (0→4), (0→5), and (0→6) $v' \rightarrow v''$ transitions. Much less intense are peaks due to transitions from $v'=1$ level. A peak at 692 nm (6→12) is fairly visible.

The emission spectrum appears to be vibrationally hot, that is significant emission is occurring from $v' \geq 1$. The vibrational temperature of the v' level can be estimated from the heights (intensities) of the emission peaks. The intensity of the emission is proportional to the population of the level multiplied by the Franck-Condon factor for that transition (3:6796). Assuming the v' level is in a Boltzmann distribution, and knowing the appropriate Franck-Condon factor, the relative intensities of the transitions can be found as a function of temperature.

The poor resolution of the spectrum made identifying the transitions difficult. Enough peaks can be identified to indicate

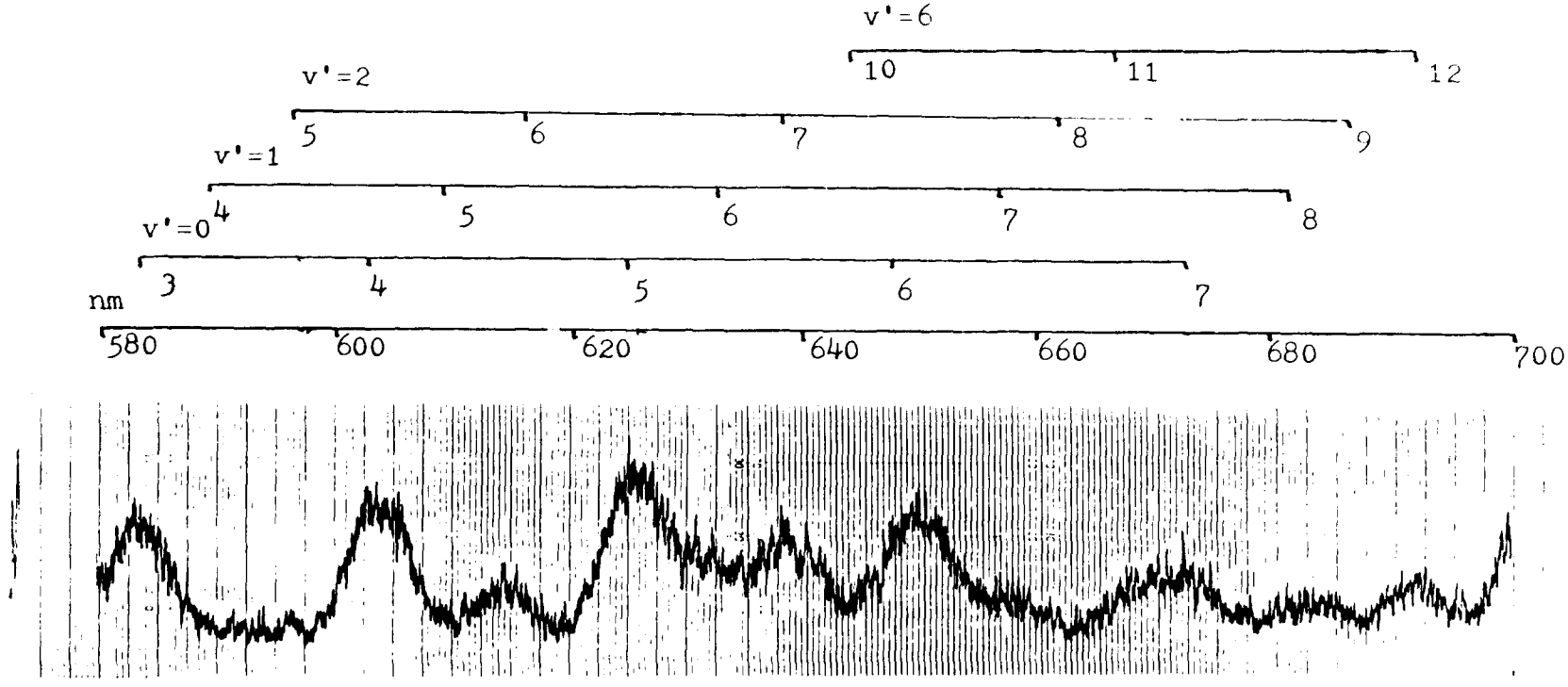

Figure 11. IF(B → X) Chemiluminescence Spectrum

the vibrational temperature of the B state is on the order of 1000 K.

The transition from v'=6 is significant in that if pumping of vibrationally cold IF is occurring due to $O_2(^1\Sigma)$ as was written in equations (1) and (2),

$$IF(X) + O_2(^1\Sigma) \rightarrow IF(A') + O_2(^3\Sigma) \quad (1)$$

$$IF(A') + O_2(^1\Delta) \rightarrow IF(B) + O_2(^3\Sigma) \quad (2)$$

then equation (2) would pump IF into the v'=6 level of the B state.

This conclusion is counter to what Lee observed using the unmodified flow apparatus (2:44-45). The original work by Davis (1:21-22) showed substantial population of the v'=6,7, and 8 levels. The IF(B) emission obtained in this research was smaller than that obtained by Lee by one half to one order of magnitude. Reasons for this may include low $[O_2(^1\Sigma)]$ (the system had been opened prior to the run which may have introduced contaminants), or the flow may have been too fast to achieve sufficient mixing prior to leaving the viewing region. The flow speed during the IF(B) reaction was about 0.7 m/sec. Flow velocity data for Lee's work is not available. Lee also used copper tubing in the singlet oxygen line, which may have removed $O_2(^1\Sigma)$, with the $O_2(^1\Delta)$ not having enough time to build up an appreciable concentration of $O_2(^1\Sigma)$. This result does indicate that $O_2(^1\Sigma)$ pumping of vibrationally cold IF to IF(A') cannot be ruled out and further study is warranted.

During this run, the system was not optimized to achieve maximum signal and further investigation would be necessary to positively identify the IF(B) emission lines. Unfortunately, the IF(B) emission was not very reproducible. This highlighted the need to characterize the system with respect to the $O_2(^1\Sigma)$ and IF precursors. At that time, the decision was made to measure the $O_2(^1\Sigma)$ quenching coefficients. This allowed a measure of how accurately the flow system could reproduce previous results taken from the literature, and demonstrated interactions between the flow system and reactant gases.

Singlet Oxygen Production

Singlet oxygen production appeared to depended strongly on whatever contamination might have been in the system. If the system had been opened to air for any appreciable amount of time (longer than a few minutes), whatever was in the air inevitably deposited itself on the system walls. On one occasion, after being opened to ambient pressure for a few hours, it took constant pumping over three days to bring the count up from 1000/second to 40,000+/second. The mercuric oxide ring had some effect on increasing $O_2(^1\Sigma)$ concentration while removing atomic oxygen. However, this effect appeared to be less than that due to preventing system contamination.

Quenching and Determination of Rate Constants

Typical data for a quenching experiment is shown in Figure 12, in this case for CF_4 gas. It was expected that the relation

between the emission intensity and $P(CF_4)$ would be linear, however two distinct regions seem to occur for this data. The steeper slope appears to give the more correct rate constant. The other gases also display this same trend to various degrees.

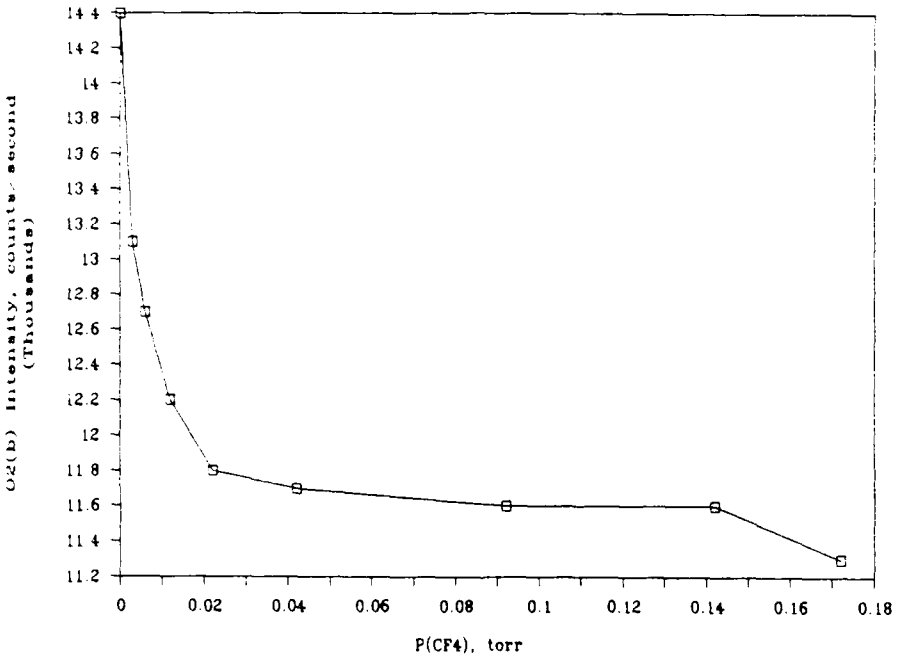

Figure 12. Relative Intensity of $O_2(^1\Sigma)$ Emission as a Function of CF_4 Partial Pressure, Increasing Pressure Increments

Change in Slope. The change of slope can be accounted for in the γ' term of equation (35).

$$S = 1 + \frac{\beta}{1 + \gamma'} \times \frac{P(M)}{P(O_2)} \qquad (35)$$

If all other rates and concentrations are assumed constant, γ' changes linearly with k_w. If the wall quenching rate changes

after being exposed to quencher gas, then γ' would change accordingly. It is likely that the quencher adheres to the wall and increases the wall quenching. As the wall is poisoned by the quencher gas to a greater degree by higher quencher pressure, γ' increases and the slope term $\beta/(1 + \gamma')$ decreases. Eventually, a point is reached where the wall becomes saturated and γ' stabilizes.

This situation would necessitate taking data over the range where the wall poisoning (and wall quenching) is at its lowest value. Data was taken at low quencher pressure, on the steep slope section of the curve.

The injection procedure was then changed to that of injecting the quencher in increments separated by a period of zero quencher pressure. A typical run for CF_4 is shown in Figure 13. The top curve is quenching of $O_2(^1\Sigma)$ due to the quenching gas and wall quenching. The bottom curve is the quenching due to $O_2(^1\Sigma)$ collisions with the "poisoned" wall (the quencher gas flow being shut off). The most notable features are again the evidence of two regions of different slopes, and the zero quencher gas curve falls below the quencher curve. On similar data taken for CO_2, the two curves cross in the region where the slope of the quenching curve changes. In this region, the zero quencher curve is above the quencher curve.

The interrupted increment technique appeared to extend the region over which "good" data points were taken. Now, the changing wall quenching effect is clearly visible. In regions

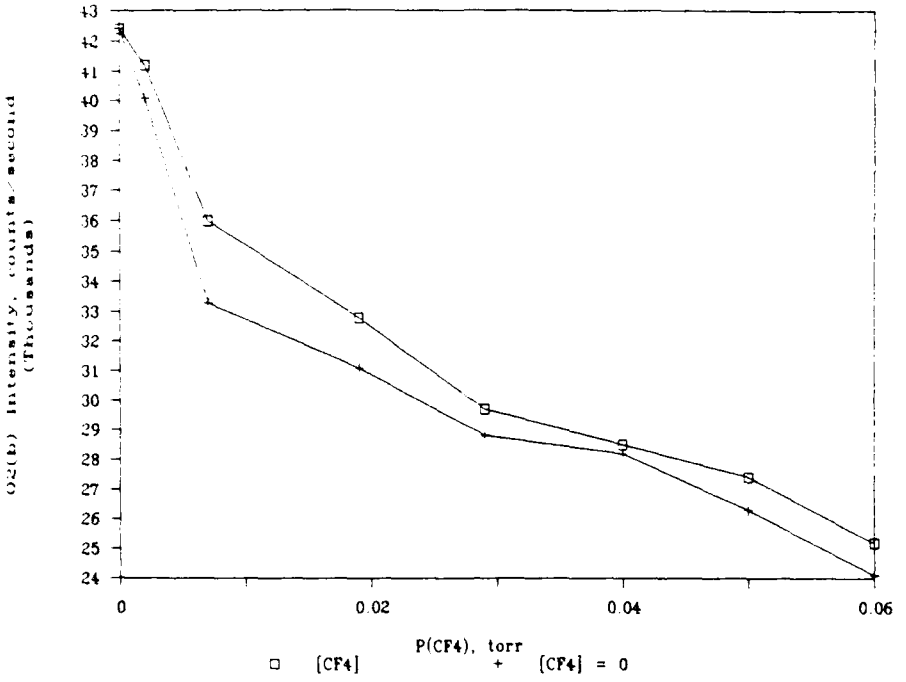

Figure 13. Relative Intensity of $O_2(^1\Sigma)$ Emission as a Function of CF_4 Partial Pressure, Interrupted Pressure Increments

where the slope is steep, the wall is continuing to be poisoned by the quencher, but the shallow slope region is where the wall has become saturated and its quenching is predominant over collisional quenching with the quencher (γ' dominating in the denominator of where the slope is steep, the wall is continuing to be poisoned by the rate equation).

The best agreement between experimental and literature values of k occurred for CF_4 and N_2. Normalized quenching data for CF_4 is shown in Figure 14. The plot shows the normalized quenching data, the points used in the linear regression to determine k'_M, and the line calculated using k'_M values taken from literature,

assuming $\gamma'=0$. By comparing the two slopes, γ' could then be experimentally determined. For the N_2 and CF_4 experiments, γ' was found to be almost zero for N_2 and 0.2 for CF_4.

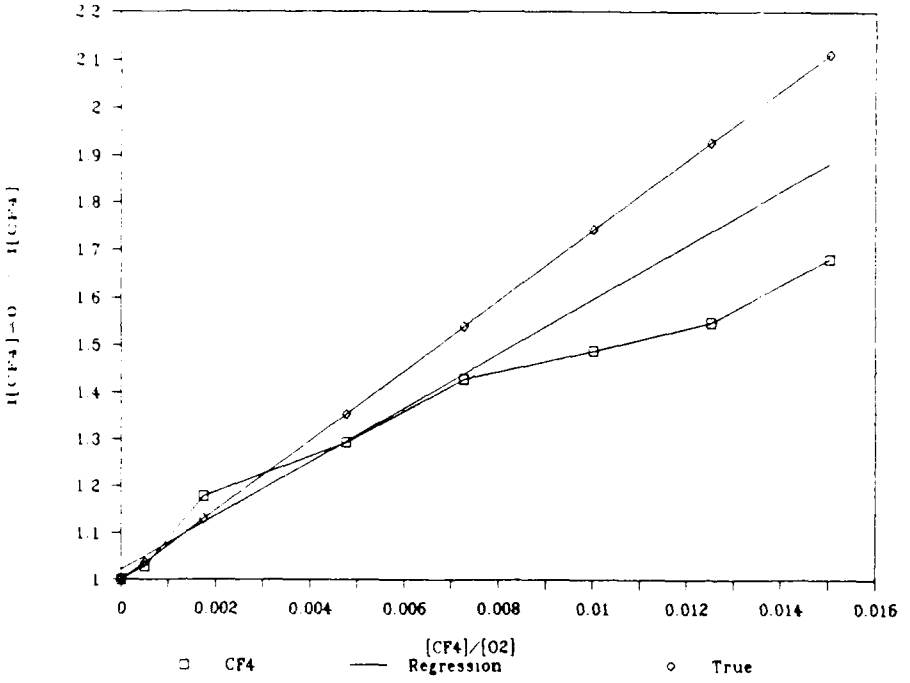

Figure 14. Normalized Intensity of $O_2(^1\Sigma)$ Emission Intensity as a Function of the Ratio of CF_4 Partial Pressure to Total O_2 Pressure

An estimate of γ' can be calculated from the wall quenching rate literature value. Earlier, k_w was defined as:

$$k_w = \frac{\bar{c}}{4}\frac{A_s}{V}\gamma \qquad (36)$$

(14, 15). Taking $\gamma=0.01$ (23:207), $A_s/V=400\ m^{-1}$, $\bar{c}/4=110\ m\ sec^{-1}$, one can calculate $k_w=440\ sec^{-1}$, and $\gamma'=125$. This value is about 10^3 larger than that determined experimentally.

The radial distribution of $O_2(^1\Sigma)$ can be between two

extremes. The first is where the molecules quickly travel throughout the tube in a laminar flow, giving a uniform distribution. This would allow the wall quenching to be essentially that determined above. The second case is where the $[O_2(^1\Sigma)]$ is determined by radial diffusion. The walls quench those $O_2(^1\Sigma)$ closest to them, but the molecules in the center of the tube cannot travel to the walls. In such a case, a concentration gradient is established, and the number of $O_2(^1\Sigma)$ molecules quenched at the wall is effectively reduced. The second case is the diffusion limited case (14).

The diffusion coefficient is given by

$$D = \frac{1}{3} \bar{c} \lambda \tag{37}$$

where λ is the mean free path. The flux due to diffusion is

$$J_{diff} = D \frac{dn}{dr} = D \frac{n_o - n_{wall}}{r} = D \frac{n_o}{r} = \frac{1}{3} \bar{c} \lambda \frac{n}{r} \tag{38}$$

where n is the number density, and r is the radial distance from the center. The above is for the limiting case of no molecules at the walls. The flux of particles hitting the wall is

$$J_w = \frac{\bar{c}}{4} \gamma n \tag{39}$$

The ratio J_w/J_{diff} is equal to k_w/k_d, where k_d is the "effective" wall rate, limited by diffusion (13). For $\gamma=10^{-2}$, one can calculate that $J_w/J_{diff}=605$, and $k_d=0.73$. This gives a $\gamma'=0.14$, which agrees with the experimental value (the uncertainty in γ is

Table I. Experimental and Literature Values of $O_2(^1\Sigma)$ Quenching Coefficients for Various Gases, cm^3 $molecule^{-1}$ $second^{-1}$

Quencher	k_M, Present Work	k_M, Previous Work	Percent Difference	Reference
CF_4	(2.0±0.5)E-15	2.6E-15	23	11:19
N_2	(2.0±0.5)E-15	2.1E-15	4.8	11:19
CF_3I	(4.4±2.4)E-15	No Data		
Microwave CF_4	(8.7±5.1)E-15	No Data		
CO_2	(1.4±0.8)E-14	3.3E-13	96	11:19
He	(1.5±0.8)E-15	1.0E-17	1.5E4	24:206

an order of magnitude) (25:89). Quenching coefficients determined for the other gases, using $\gamma'=0.1$, are given in Table I. Error bounds were determined from statistical analysis of the propagation of error.

In Figure 13, the $O_2(^1\Sigma)$ quenching due to collisions with the poisoned wall (quencher gas flow shut off) appears to be greater than when the quencher gas was in the system. This would seem to indicate that quenching in the system became greater after the quenching gas was removed. The region after the crossover on the CO_2 curve displays the expected characteristic of the system quenching being less for the zero quencher condition. However, this is in the region where the shallow slope occurs. It was found that the "poisoned" wall quenching being greater than the quenching due to the quenching gas occurred at the beginning of a quenching experiment. An experiment was run where the quencher gas was introduced in uninterrupted increasing amounts (without returning to zero) until the quenching was in the shallow slope region of the quenching curve. From that quencher gas partial pressure, the quencher gas was then introduced in interrupted increments which returned to the "zero" point of the last pressure prior to starting the interrupted increments. The quenching curve then continued with the existing shallow slope. This suggests that the two slope characteristic of the quenching curve is due to the poisoning of the wall (and changing the quenching coefficient) rather than the technique of using interrupted pressure increments.

The "poisoned wall" quenching curve falling below the curve for the quenching gas could be attributed in part to: 1) the oxygen pressure being less than its original pressure prior to any addition of quencher (the balance of the pressure being residual quencher); 2) the valve on the quencher flowmeter may not have been fully shut off; 3) degassing of quencher from the tubing walls which adds to the total flow; 4) some fraction of O_2 being used to condition the tubing walls after the quencher is shut off and being lost from the total O_2 flow.

Points 1) and 2) are both possible, especially as the flowmeter readings vary as additional gases are added or removed. The response of the flowmeters is such that there is some time lag involved. Point 3) is also possible, although attempts to measure the effect of outgassing were not successful. Point 4) may be true, especially in light of $O_2(^1\Sigma)$ reactivity. When initially turned on, the $O_2(^1\Sigma)$ emission would increase over time, possibly indicative of the walls accommodating the O_2 flow.

Outgassing and Quencher Gas-Wall Reactions. Results for quencher-wall reaction and outgassing were inconclusive. In these experiments, the pressure was monitored over a period of time for the three cases of the system evacuated prior to addition of quencher gas, filled with quencher gas, and re-evacuated of the quencher gas. An increase in the system pressure would be due to leaks in the system and wall absorption or outgassing of the quencher gas. A decrease in the rate of pressure rise for the filled system would have indicated the quencher gas was attaching

to the walls. An increase in the rate of pressure rise for the re-evacuated system would have indicated degassing of the walls. Gases that were not exposed to the microwave cavity (CO_2, CF_4, and CF_3I) showed none of the above trends. At least with this apparatus, there was no discernible change in the rate of the pressure rise for the three cases. The microwave CF_4 showed strong evidence of attaching to the non-passivated walls of the system. This was to be expected, and the reactivity of microwave CF_4 to passivated tubing may be different. At least for the technique used in this work, accommodation and outgassing do not appear to be significant reactions in non-microwave excited gases. Data for the CF_4 alone and those for the microwave CF_4 are shown in Figures 15 and 16.

Conclusions

Data obtained in this thesis research suggests that in the cold IF pumping reaction, the IF(A') state may indeed be an intermediate state. This is based on the vibrationally hot IF(B) emission that was observed, and the possible emission originating from the v'=6 vibrational level.

In light of the above discussion of an increasing wall quenching effect, the $O_2(^1\Sigma)$ quenching data by Lee needs to be re-examined. His quenching runs were done in increments of 0.07 torr to total quencher pressures of 1.4 torr or greater. Data from this work indicate that wall quenching effects predominate at quencher pressures greater than 0.01 torr. Lee's quenching experiments began in a regime where wall quenching had already

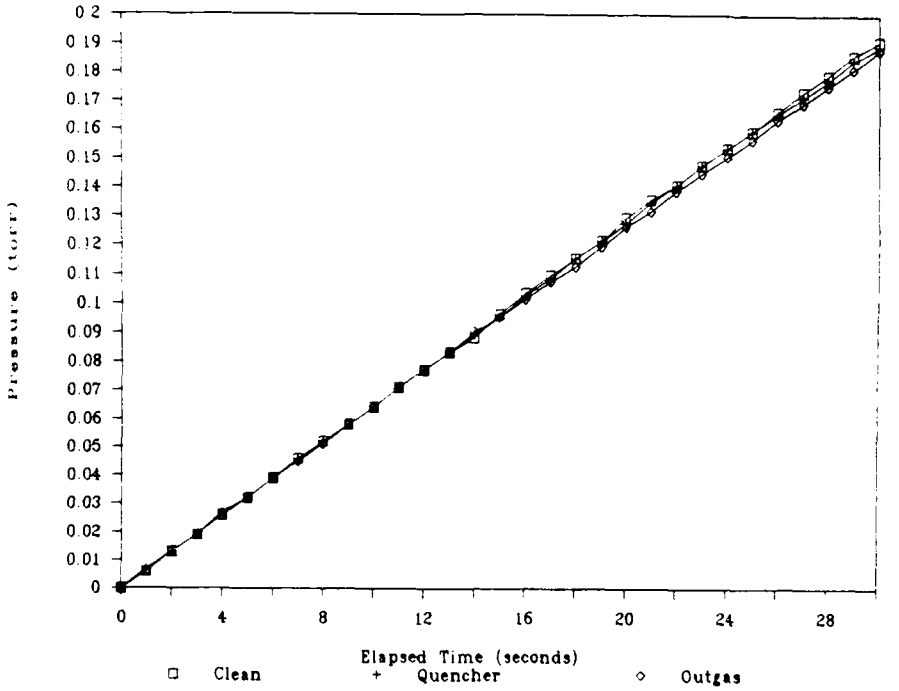

Figure 15. Comparison of Pressure Increase in Reaction Chamber Due to System Leaks verses System Leaks + CF_4 - Wall Reaction

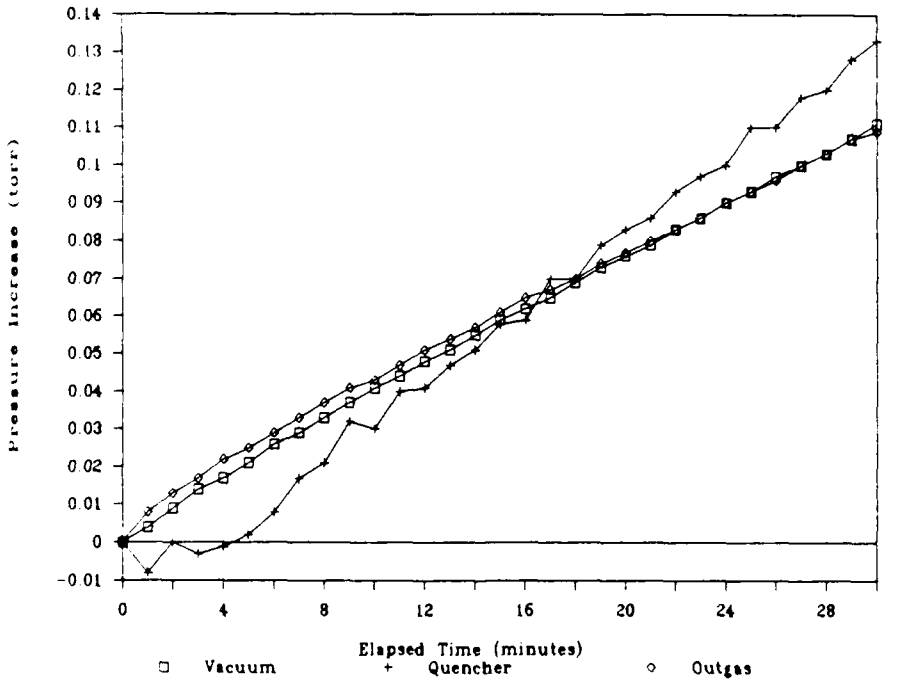

Figure 16. Comparison of Pressure Increase in Reaction Chamber Due to System Leaks verses System Leaks + Microwave CF_4 - Wall Reaction

become dominant in the $O_2(^1\Sigma)$ quenching process.

Wall reactions may become significant in kinetics studies from several standpoints. The wall poisoning issue previously discussed indicates how drastic the wall rate may change, even at low levels of quencher gas. Additionally, it is imperative to characterize the apparatus in terms of the flow and its reaction with the species present. Case in point is the diffusion limited reaction which reduced the "effective" γ' wall quenching term in the relative rate equation.

One way to minimize the changing wall rate problems is optimize the system design. Davis had also determined a quenching coefficient for CO_2 quenching of $O_2(^1\Sigma)$ that agreed with previous literature values (1:15). Davis used a larger diameter flow tube, coated with Teflon. Both of these factors would reduce the wall quenching of $O_2(^1\Sigma)$.

VI. Recommendations

The work to determine rate constants for IF and its precursors ought to be continued. There are a number of recommendations to be made for the future work in this area. These are listed in terms of relative importance (as viewed by this researcher).

The six-way cross flowing reactor ought to be replaced with a flow tube. The current system is limited to a steady state condition of the reaction. Multiple viewing ports are required to monitor the evolution of the IF(B) pumping or $O_2(^1\Sigma)$ quenching. The ability to monitor the initial $O_2(^1\Sigma)$ emission prior to addition of the quencher, and then again after the gas mix has come to equilibrium would improve the accuracy of this work. Additionally, using a flow tube would reduce the problem of wall poisoning due to the quencher gas (the ratio of A_s/V would decrease for a larger diameter tube).

Digital flowmeters are needed for the precise control of the gases that are required for this rate determination work.

A new, calibrated Baratron manometer (300 series) would aid in attaining greater accuracy in pressure measurements.

Incorporating Teflon tubing or coatings in the system tubing after the microwave cavities would decrease the wall quenching effects. In turn, this would increase the range over which data could accurately be taken, again increasing the accuracy of the measurements. If this isn't practical, then a second option would

be to coat the system tubing after the microwave cavity with halocarbon wax ($\rho = 10^{-3}$) (16:454).

If CF_3I will be used in the future for the IF production, some purification work ought to be done to see what effect contaminants in the gas have on the quenching rate. The I_2 contaminant should be trapped out by incorporating an ice bath cold trap in the CF_3I line.

Data on the rate constants for IF and its precursors do exist for some of the reactants. For example, Davis calculated a lower value for k_{IF} of the $O_2(^1\Sigma)$ + IF reaction of 1.7×10^{-15} $cm^3/(molecule\ sec)$ (1:31). This value was a lower limit, and a more accurate value has not been determined. Specific measurements for the future might include:

characterization of the microwave CF_4 flow

obtaining a better estimate of the $O_2(^1\Sigma)$ wall quenching rate (realizing that such a number would be highly dependent on wall cleanliness)

assuming the wall poisoning problem could be minimized, a study of varying the ratio of microwave CF_4 to CF_3I would be beneficial in finding an optimum stoichiometry.

Even in the event that the IF laser is surpassed by another system, such measurements would still be valuable in predicting or explaining performance of other potential laser candidates.

Bibliography

1. Davis, S. J., et al. Chemical Pump Sources for IF(B) AFWL-TR-87-92: Final Report. Contract F29601-86-C-0017. Kirtland AFB NM: Air Force Weapons Laboratory, May 1987.

2. Lee, Capt William M. Collisional Energy Transfer Mechanisms AFIT/GE/ENP/88D-3. School of Engineering, Air Force Institute of Technology (AU), Wright-Patterson AFB OH. December 1988.

3. Whitefield, P. D., R. F. Shea, and S. J. Davis. "Singlet molecular oxygen pumping of IF $B^3\Pi(0^+)$," Journal of Chemical Physics, 78: 6793-6801 (1 June 1983).

4. Johnson, 1Lt Ray O. Study of the Energy Transfer Mechanisms between $O_2(a)$ and Iodine Monofluoride. MS Thesis, AFIT/GE/ENG/87D-27. School of Engineering, Air Force Institute of Technology (AU), Wright-Patterson AFB OH, December 1987.

5. Trickl, T. and J. Wanner. "The Dynamics of the Reactions F + IX $\rightarrow$ IF + X (X = Cl, Br, I): A Laser-Induced Fluorescence Study," Journal of Chemical Physics, 74: 6508 (1981).

6. Stein, L., J. Wanner, and H. Walther. "Laser Induced Fluorescence Study of the Reactions of F Atoms with CH_3I and CF_3I." Journal of Chemical Physics, 72: 1128 (January 1980).

7. Roh, Won B. Professor, Physics Department, Air Force Institute of Technology. Personal Interviews. AFIT, Wright-Patterson AFB OH, December 1988 through September 1989.

8. Herzberg, Gerhard. Spectra of Diatomic Molecules. New York: Van Nostrand Reinhold Company, 1950.

9. Kolb, C. E. and M. Kaufman. "Molecular Beam Analysis Investigation of the Reaction between Atomic Fluorine and Carbon Tetrachloride," Journal of Physical Chemistry, 76: 947-953, (30 March 1972).

10. Wasserman, H. H. and R. W. Murray Singlet Oxygen. New York: Academic Press, 1979.

11. Rånby, B. and J. F. Rabek. Singlet Oxygen. New York: John Wiley and Sons, Inc., 1979.

12. Frost, A. A. and R. G. Pearson. Kinetics and Mechanisms. New York: John Wiley and Sons, Inc., 1953.

13. Masterton, W. L. and E. J. Slowinski. Chemical Principles (Fourth Edition). Philadelphia: W.B. Saunders Co., 1977.

14. Perram, Capt Glen P. Professor, Physics Department, Air Force Institute of Technology. Personal Interviews. AFIT, Wright-Patterson AFB OH, June 1989 through September 1989.

15. Perram, Capt Glen P. and G. D. Hager. The Standard Chemical Oxygen-Iodine Laser Kinetics Package AFWL-TR-88-50. Air Force Weapons Laboratory (AFSC), Kirtland AFB NM, October 1988.

16. Heidner III, R. F. "Behavior of Singlet Oxygen in the Oxygen-Iodine Transfer Laser," Journal of Photochemistry, 25: 449-463 (1984).

17. Airco R. & S.G. Flowmeter Calibration Tables.

18. Catalog 84. Matheson Gas Products, Twinsburg OH, 1984.

19. Piper, L. G. et al. Kinetics of Iodine Monofluoride Excitation by Energetic Nitrogen AFWL-TR-84-156. Contract F29601-83-C-0051. Kirtland AFB NM, Air Force Weapons Laboratory, October 1985.

20. Johnson, Dan. WL/ARDJ, Kirtland AFB NM. Private Communication, 13 June 1989.

21. Smith, Greg. AFIT/ENP, Wright-Patterson AFB OH. Private Communication, September 1989.

22. Photomultiplier C310134. Product Literature. RCA, Electro Optics and Devices Division, Lancaster PA 17604.

23. Davis, Steven J. Telephone Interview. Physical Sciences Inc, Andover MA. Private Communication, 16 Aug 1989.

24. Setser, D. W. Reactive Intermediates in the Gas Phase. New York: Academic Press, 1979.

25. Izod, T. P. J. and R. P. Wayne, "The formation, reaction and deactivation of $O_2(^1\Sigma_g^+)$," Proceedings of the Royal Society of London, 308: 81 (1968).

Vita

Captain Robert T. [redacted] He graduated from high school in Ross, Ohio in 1980 and received an appointment to the United States Air Force Academy, from which he received the degree of Bachelor of Science in Chemistry in May 1984. Upon graduation, he received a commission into the USAF. He was assigned to HQ Foreign Technology Division as a Laser Technology Analyst until entering the School of Engineering, Air Force Institute of Technology, in June 1988.

[redacted]

UNCLASSIFIED

SECURITY CLASSIFICATION OF THIS PAGE

REPORT DOCUMENTATION PAGE

1a REPORT SECURITY CLASSIFICATION UNCLASSIFIED	1b RESTRICTIVE MARKINGS
2a SECURITY CLASSIFICATION AUTHORITY	3 DISTRIBUTION / AVAILABILITY OF REPORT Approved for public release; distribution unlimited
2b DECLASSIFICATION / DOWNGRADING SCHEDULE	
4 PERFORMING ORGANIZATION REPORT NUMBER(S) AFIT/GEP/ENP/89D-8	5 MONITORING ORGANIZATION REPORT NUMBER(S)
6a NAME OF PERFORMING ORGANIZATION School of Engineering 6b OFFICE SYMBOL (If applicable) AFIT/ENP	7a NAME OF MONITORING ORGANIZATION
6c ADDRESS (City, State, and ZIP Code) Air Force Institute of Technology Wright-Patterson AFB OH 45433-6583	7b ADDRESS (City, State, and ZIP Code)
8a NAME OF FUNDING / SPONSORING ORGANIZATION 8b OFFICE SYMBOL (If applicable)	9 PROCUREMENT INSTRUMENT IDENTIFICATION NUMBER
8c ADDRESS (City, State, and ZIP Code)	10 SOURCE OF FUNDING NUMBERS PROGRAM ELEMENT NO / PROJECT NO / TASK NO / WORK UNIT ACCESSION NO

11 TITLE (Include Security Classification)
SINGLET OXYGEN AND IODINE MONOFLUORIDE COLLISIONAL ENERGY TRANSFER MECHANISM

12 PERSONAL AUTHOR(S)
Robert T. Mack, B. S., Capt, USAF

13a TYPE OF REPORT	13b TIME COVERED	14 DATE OF REPORT (Year, Month, Day)	15 PAGE COUNT
MS Thesis	FROM _____ TO _____	1989 December	66

16 SUPPLEMENTARY NOTATION

17 COSATI CODES			18 SUBJECT TERMS (Continue on reverse if necessary and identify by block number)
FIELD	GROUP	SUB-GROUP	Singlet Oxygen Iodine Monofluoride (IF) Chemiluminescence
20	05		
07	05		

19 ABSTRACT (Continue on reverse if necessary and identify by block number)

Title: SINGLET OXYGEN AND IODINE MONOFLUORIDE COLLISIONAL ENERGY TRANSFER MECHANISM

Thesis Chairman: Won B. Roh
Professor of Engineering Physics

20 DISTRIBUTION / AVAILABILITY OF ABSTRACT ☐ UNCLASSIFIED/UNLIMITED ☒ SAME AS RPT ☐ DTIC USERS	21 ABSTRACT SECURITY CLASSIFICATION UNCLASSIFIED
22a NAME OF RESPONSIBLE INDIVIDUAL Won B. Roh	22b TELEPHONE (Include Area Code) (513) 255-4498 22c OFFICE SYMBOL AFIT/ENP

DD FORM 1473, 84 MAR 83 APR edition may be used until exhausted
All other editions are obsolete.

SECURITY CLASSIFICATION OF THIS PAGE

UNCLASSIFIED

Abstract

The reaction between singlet oxygen ($O_2(a)$ and $O_2(b)$) and iodine monofluoride (IF) occuring in a flowing reactor was observed as a means to study the energy transfer mechanism between these two molecules. Several researchers have demonstrated that singlet oxygen will efficiently pump IF(X) to the IF(B) state, however the exact mechanism has not been determined. The purpose of this research was twofold. First is to identify IF(B) emission due to pumping by $O_2(b)$. Second is to determine $O_2(b)$ quenching rate constants for IF and its precursors via measuring the decrease in the $O_2(b)$ emission intensity as a function of the concentration of the individual reactants. The IF(B) emission spectrum indicates that $O_2(b)$ pumping of IF(X) to the IF(A') state cannot be discounted. Quenching coefficients for IF precursors are presented and compared to literature values.